

Effects of spatial discretization on the simulation of surface water features in groundwater flow models

Saeed Ghaderi

Supervisors:

Professor Okke Batelaan

Dr Etienne Bresciani

Thesis submitted in partial requirement for the degree of Master of Sciences in
Water Resources Management in the School of Environment,
Faculty of Science and Engineering

May 2017



Contents

Summary	I
DECLARATION	II
Acknowledgements	III
1. Introduction	4
2. Theory and Method.....	8
2.1. Conceptual Model and Exact Solution.....	8
2.2. Numerical Model.....	9
2.3. Three-cell Model Solution	12
2.4. Error Definition	14
2.5. Equivalent Parameter.....	16
3. Results.....	17
3.1. Effects of Horizontal Discretization	17
3.2. Effect of River Position.....	22
3.3. Equivalent parameter and the river geometry.....	27
3.4. Equivalent parameter and river location.....	30
4. Discussion and Recommendations	34
4.1. Effects of spatial discretisation on GW-SW exchange.....	34
4.2. Suitability of the equivalent parameter approach	35
4.3. Limitations of the study.....	35
4.4. Ways forward	36
5. Conclusion.....	37
References	38
Appendix	40
Mflab Script.....	40

List of Figures

Figure 1. Cross sectional representation of the conceptual model from Anderson (2005)	8
Figure 2. Representation of fine spatial discretization of the model domain.....	10
Figure 3. Schematic representation of a fine horizontal discretization of the setting Error! Bookmark not defined.	
Figure 4. Schematic representation of a coarse horizontal discretization of the setting ('three-cell model') Error! Bookmark not defined.	
Figure 5. Schematic representation of the numerical setting when the river occupies some river cells fully while other partly.	15
Figure 6. Variations in error in response to horizontal discretization for different river geometries a) D/H=0.2; b) D/H=1; c) D/H=5.....	21
Figure 7. Error variation in response to the location of the river in the numerical cell	26
Figure 8. Streambed conductance as an equivalent parameter in the three-cell context for $b/dx=0.5$	29
Figure 9. Effects of river position on equivalent parameter.....	33

Summary

Interaction between groundwater and surface water is an integral part of regional groundwater models. Effective representation of surface water features can improve the accuracy of the groundwater model's ability to produce exchange values and correspondingly inform water resources managers and policy makers to make more effective decisions.

In regional models, it is common to deal with cases where there is a dimensional difference between the river and the underlying cell. Moreover, the stream is assumed to be in the centre of the finite difference cell, which might not be representative of the physical reality. The primary focus of this study is to investigate the impacts of horizontal discretization and river position on groundwater-surface water exchange quantification. This is achieved by comparing an exact analytical solution to a numerical version of an identical setting.

The exchange between the river and aquifer is classically estimated using riverbed conductance, but due to difficulties in measuring the parameters it is treated as an equivalent parameter and achieved through model calibration. This approach makes the riverbed conductance dependant on flow conditions and limits the predictive capabilities of the calibrated model. The secondary objective of this study is to investigate the suitability of the equivalent parameter approach and to observe how it functions in response to variations of other parameters.

From the first analysis, it was found that the errors induced to the model from horizontal discretization is minor and dominated by the errors from vertical coarsening for narrow rivers, but for wider rivers the errors from horizontal discretization were found to be significant. Secondly, it was shown that the maximum error occurs when the stream is attached to the border of the river cell, which is possibly due to the inability of the numerical model to capture the vertical flows in these arrangements. Also, it is shown that the equivalent conductance can vary as a function of several parameters, such as regional flows, river geometry, horizontal discretization and the location of river, the influence of which needs to be taken into consideration when defining riverbed conductance. The findings of this analysis show that the accuracy of the model output could be improved through the implementation of a riverbed conductance definition that adopts the dependence on regional flows and is also dependent on the scale of the cell.

DECLARATION

I certify that this thesis does not incorporate without acknowledgment any material previously submitted for a degree or diploma in any university; and that to the best of my knowledge and belief it does not contain any material previously published or written by another person except where due reference is made in the text.

Signed.....
Saeed Ghaderi

Date.....
29 May 2017

Acknowledgements

I would like to thank Dr Etienne Bresciani for your time, patience, constant involvement and providing constructive feedbacks throughout the year. I am gratefully indebted to his guidance and insightful comments during this research. I cannot have imagined having a better mentor and advisor for my thesis and I look forward to opportunities to work with you again in the future.

I would also like to express my sincere gratitude to Professor Okke Batelaan for his constructive feedbacks and continuous support throughout my study. I have gained a lot from his extensive knowledge.

To my parents, thanks for providing the once in a lifetime opportunity of studying in Australia and your endless support and encouragement throughout all years of my study to this point. Your unconditional love and support will never be forgotten.

Finally, I would like to thank my partner Foroogh for providing me with unfailing support, sacrifices and continuous inspirations throughout my study. I wouldn't have finished this thesis without you.

1. Introduction

The significance of groundwater-surface water (GW-SW) interaction has been accentuated in the past decades by the attentions upon groundwater-dependent ecosystems and environmental flows, water quality, and importance of water rights and water allocations (Sophocleous, 2002, Brunke and Gonser, 1997, Fleckenstein et al., 2010). Interactions between groundwater and surface water occur in most landscapes varying from streams, creeks and lakes to river valleys and the coast (Winter, 1999). However, due to complexities and difficulties in measuring GW-SW exchange, these interactions were often disregarded in management practices in the past (Winter et al., 1998).

For integrated management of water resources, and quantification of the exchange processes in the hydrological cycle, particularly when GW-SW interaction is of concern, it is vital to assess the resources at the catchment or regional scale (Aeschbach-Hertig and Gleeson, 2012). The scale and complexity of water management issues at a regional scale have increasingly highlighted the significance of using numerical models (Zhou and Li, 2011). Presently, groundwater models offer a common way of dealing with regional groundwater problems. However, developing such models is challenging. Namely, the large extent of the model domains, and the limitation of data and computational restrictions constrain the practitioners to use temporally and spatially low resolution models (Fleckenstein et al., 2010, Barthel and Banzhaf, 2016). Various field techniques are available in the literature for measuring GW-SW exchange at the local scale (Kalbus et al., 2006). However, there is a disconnection between field-based hydraulic parameters and parameterizing regional scale models (Snowdon and Craig, 2016, Vermeulen et al., 2006). Due to difficulties of measuring the hydraulic properties in the field, many parameters are often oversimplified or assumed as homogeneous (Irvine et al., 2012, Goderniaux et al., 2009).

MODFLOW (Harbaugh, 2005), the industry standard code for numerical groundwater flow modelling, allows the modeller to simulate groundwater flow in three dimensions; however, a single-layer approach is typically adopted to describe the upper aquifer. By doing so, flow is assumed to be horizontal within that aquifer. The exchange flux between the upper aquifer and surface water bodies are then modelled by using packages such as RIV (Harbaugh, 2005), STR (Prudic, 1989), SFR (Prudic et al., 2004), LAK (Merritt and Konikow, 2000) and RES (Fenske et al., 1996) within which the vertical head loss between the water body and the aquifer is assumed to occur solely across the riverbed, conceptualized as a low-conductivity layer (the so-called “clogging layer”). Within those packages, the clogging layer is expressed by the physical dimensions and hydraulic conductivity of the clogging layer, aggregated to a single parameter called

streambed conductance. However, in many cases, the clogging layer might be ineffective or there might be no clogging layer at all, in which case significant head losses occur within the aquifer itself (Rushton, 2007, Morel-Seytoux et al., 2014). Furthermore, the horizontal discretization used in numerical models is typically coarse relative to the dimension of rivers (Brunner et al., 2010, Mehl and Hill, 2010). This introduces computational errors, an issue that is especially critical in regional scale models. Furthermore, there is little guidance in the literature to deal with situations when multiple surface water features are located within one cell (De Lange, 1999, Snowdon and Craig, 2016).

As a consequence of the above conceptual and computational limitations, the computed streambed conductance poorly represents the physical reality of the setting. In practice therefore, the conductance is treated as a fitting parameter which is obtained through model calibration to flow or head observations (Irvine et al., 2012, Rushton, 2007, Liggett et al., 2012, Rassam and Werner, 2008). This process makes the exchange coefficient (i.e. the calibrated conductance) dependent on various parameters such as the flow conditions for which the model is calibrated, and therefore limits the predictive capabilities of the model (Anderson, 2005).

Local grid refinement methods can directly address the issues by allowing the use of finer grid resolution around surface water bodies while keeping a coarse grid resolution away from them (Mehl and Hill, 2005). However, applying this method in areas with abundance of surface-water features can imply a significant computational burden to the model, particularly when there is a dense drainage network. Vilhelmsen et al. (2012) showed that local grid refinement can be less efficient than global refinement when the refined area is considerable in size, for instance, a quarter of the model domain. In addition, the physical reality of a streambed and its vicinity is unlikely to be thoroughly represented even with a very fine discretization (Rushton, 2007).

Alternatively, Morel-Seytoux (2009), Morel-Seytoux et al. (2014), Miracapillo and Morel-Seytoux (2014) and Morel-Seytoux et al. (2016) proposed to embed an analytical solution in the numerical model to solve more accurately and efficiently groundwater flow near the rivers. Available analytical solutions are two-dimensional in a vertical cross section perpendicular to the river, and can consider several parameters such as degree of penetration of the river in the aquifer, river wetted area and aquifer anisotropy. However, available analytical solutions are still limited in terms of the geometry and heterogeneity of hydraulic conductivity they can handle, and they neglect the effects of the third dimension. Furthermore, this approach requires a special arrangement of cells neighbouring the stream, making it difficult to deal with cases where multiple streams or meandering rivers occur (Pauw et al., 2015).

Cousquer et al. (2017), presented a method by which estimations of riverbed conductance for a coarse horizontal model is calculated from a fine cross-sectional numerical version of the same model. Their method considers the impacts of aquifer properties and model discretization. Their methodology, however, assumes a linear correlation between the exchange rate and river-aquifer head differences.

Anderson (2005) argued that a one-parameter equivalent model of the aquifer-stream exchange (i.e. the classical clogging layer conceptualization) is unable to represent the 3D nature of groundwater flow dynamics underneath the stream. Consequently, Anderson (2005) introduced a two-parameter equivalent model of the aquifer-stream exchange in a 1D Dupuit-based analytical solution. In this model, one parameter represents a clogging layer (as classically, even though there may not be any clogging layer at all) and the second parameter represents a fictitious heterogeneity of hydraulic conductivity in the aquifer underneath the stream. Calibration of these two parameters was shown to yield unique values that are independent of the flow conditions, thus ensuring the predictability of the model. This approach, as opposed to local grid refinement and the Morel-Seytoux (2009) solution, sacrifices the thorough physical reality, but the implied distortion from physical reality was shown to be relatively minor (Anderson, 2005). This method, however, has not been tested in a numerical model.

The first objective of this work is to carry out a rigorous evaluation of the errors introduced by the horizontal discretization in the simulation of groundwater-surface water interactions in numerical models. Of interest is a better understanding of the origin and magnitude of these errors. Different parameters influencing the error are characterized and the extent to which these parameters can alter the error are analysed. Mehl and Hill (2010) previously studied the effects of grid resolution on the river-aquifer exchange, but their method did not consider an extended range of river and cell arrangement as in this study. Also, their method complexity does not reflect the parameters that control the errors and their magnitude of influence.

The second objective is to evaluate the suitability of the clogging layer conceptualization to be an equivalent model. Anderson (2005) previously showed that the equivalent models depend on flow conditions, making them ineffective for flow conditions other than the calibration condition. Their method assesses the equivalent model in an analytical context, while in this study, a numerical approach is adopted to evaluate the effectiveness of the equivalent model as a function of grid size and position of river within grid cells.

The robust evaluation of errors done in this study should provide a roadmap for modellers to differentiate the situations in which the error is significant from the situations in which the error may be negligible. Consequently, one could either avoid those circumstances (e.g. by choosing an appropriate spatial discretization) or at the very least discern what the model can or cannot do. The other major significance of

this study is to identify the parameters that have the strongest control of the error, such that their effects can be accounted for in future developments of more effective conceptualizations.

2. Theory and Method

2.1. Conceptual Model and Exact Solution

Following Anderson (2005), we consider an infinite strip of an aquifer in a 2D vertical cross section perpendicular to a river. The aquifer of thickness H [L] is confined except along the river, and is in a steady state condition. The river of width D [L] is assumed to be in direct contact with the underlying aquifer (i.e. there is no clogging layer between the river and the aquifer) with the exchange rate of Q_{riv} . A schematic representation of the analytical setting is depicted in Figure 1.

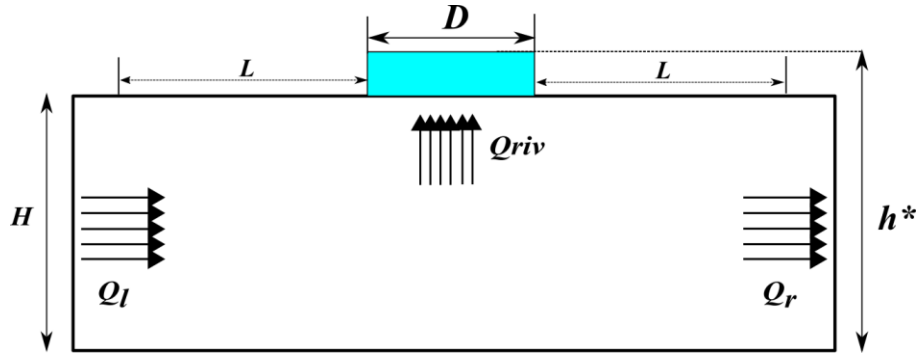


Figure 1. Cross sectional representation of the conceptual model from Anderson (2005)

Anderson (2005) developed an exact (2D) analytical solution for this problem, from which heads at a distance L [L] from the right and left edges of the stream and can be calculated as:

$$(h_r)_{Exact-Analytical} = -\frac{Q_r L}{KH} + \frac{Q_r}{K\pi} \ln\left(\frac{1}{4}(1-\gamma)\right) - \frac{Q_l}{K\pi} \ln\left(\frac{1-\gamma^{0.5}}{1+\gamma^{0.5}}\right) + h^* \quad (1)$$

$$(h_l)_{Exact-Analytical} = \frac{Q_l L}{KH} + \frac{Q_r}{K\pi} \ln\left(\frac{1-\gamma^{0.5}}{1+\gamma^{0.5}}\right) - \frac{Q_l}{K\pi} \ln\left(\frac{1}{4}(1-\gamma)\right) + h^* \quad (2)$$

Where $(h_r)_{Exact-Analytical}$ [L] and $(h_l)_{Exact-Analytical}$ [L] are the heads at a distance L [L] from the right and left stream edges, Q_l [$L^2 T^{-1}$] and Q_r [$L^2 T^{-1}$] are regional fluxes entering left and exiting right of the model domain, respectively, K [$L T^{-1}$] is the hydraulic conductivity of the aquifer, h^* is the river stage [L] and γ [-] is defined as:

$$\gamma = \exp\left[-\pi \frac{D}{H}\right] \quad (3)$$

Equation (1) and (2) is only valid for $L/H > 1.5$ (Anderson, 2005), and following Anderson (2005), we assign $L = 2H$ as a minimum distance from the river edge to the point where the head is calculated. Here we refer to this minimum distance as the *far distance*. The far distance implies that the Dupuit assumption is valid at and beyond this point (Anderson, 2005), which explains why equation (1) and (2) do not depend on the position along the z axis. Similar terminology has been used in literature to describe the distance beyond which the Dupuit assumption is valid by Haitjema (1987), Morel-Seytoux et al. (2016), and Cousquer et al. (2017).

2.2. Numerical Model

In numerical groundwater flow models, the model domain is discretised both in vertical and horizontal directions, as shown in Figure 2. Based on the modelling objectives, modellers typically choose the grid resolution at one of the primary stages of model development (Anderson et al., 2015). Discussion of the effect of vertical discretization has been previously investigated both analytically (Anderson, 2005), and using numerical methods (Mehl and Hill, 2010). Therefore, this study primarily focuses on the influence of horizontal discretization. The numerical model will thus have a single layer throughout this study, reflecting a common situation in practical applications. This case represents the extreme case of coarse vertical discretization. Schematically the model domain discretization is simplified as in **Error! Reference source not found.**

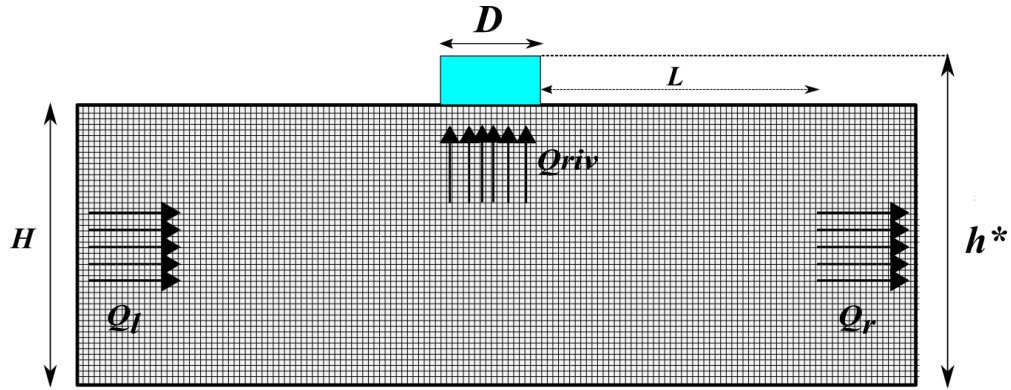


Figure 2. Representation of fine spatial discretization of the model domain

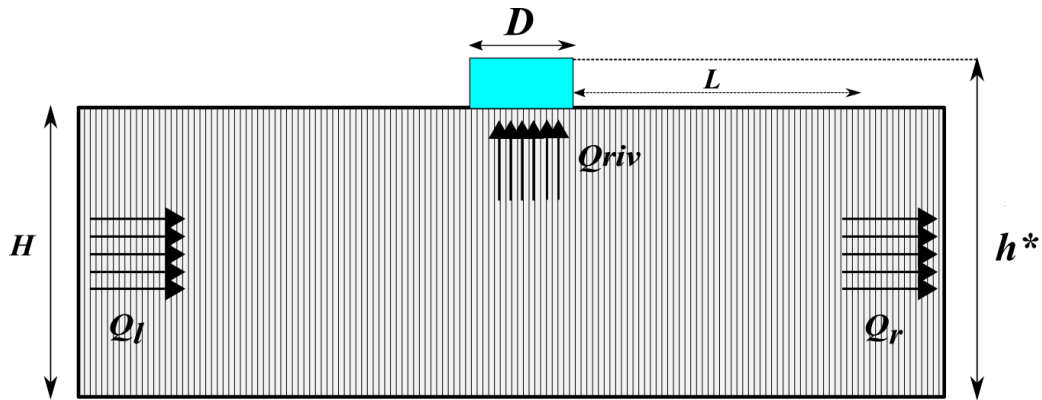


Figure 3. Schematic representation of a fine horizontal discretization of the setting

Error! Reference source not found. represents a very high horizontal resolution of the model domain in which the river is covered by numerous cells throughout its width. In regional numerical models however, it is common to deal with river widths smaller than the cell size (Brunner et al., 2010, Mehl and Hill, 2010, Morel-Seytoux et al., 2016). In this study, we will study the effect of horizontal resolution by varying the grid step from sizes significantly smaller than the river (as illustrated in **Error! Reference source not found.**) to sizes significantly larger than the river. **Error! Reference source not found.** schematically displays a regional version of the numerical model in which the river cell is considered together with one cell on the left and one cell on the right. This configuration is referred to as the ‘three-cell model’.

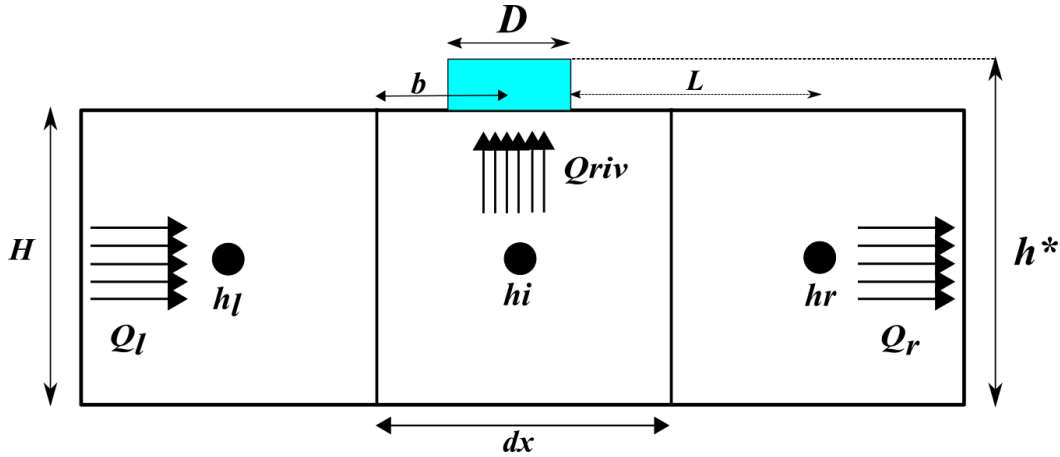


Figure 4. Schematic representation of a coarse horizontal discretization of the setting ('three-cell model')

The numerical model produces head values at the calculation nodes distance of which should always be greater than the far distance condition ($2H$), such that the far distance condition is met. Therefore, we evaluate the head in the first cell adjacent to the river, centre of which is farther than the far distance. As such, depending on the horizontal discretization of the cell, a variable number of cells is created (either on the left or right side of the river) until the far distance condition becomes valid in the centre of one cell. In this study, only the heads at the right side of the river are evaluated, but the method is also applicable for evaluating the head values on the left side of the domain.

An additional parameter, b [L], is introduced to study the impacts of stream position relative to the grid. Precisely, b indicates the distance from the left border of the cell that contains the centre of the river to the centre of the river, as shown in **Error! Reference source not found.** for the three-cell model and in Figure 5 for a more generic case. The location of the river in the cell is then incorporated in calculating the distance from the edge of the river to the point where head is calculated. This distance will be the distance at which the solution will be evaluated by comparing the numerical solution to the exact solution, i.e. this distance is L in equations (1) and (2).

The finite difference groundwater flow model, MODFLOW 2005, used to simulate the flow equation, within which Q_r and Q_l are assigned by using a specified flux boundary condition (WEL package) at the last cell on the left and the right of the model domain. The RIV package is used to simulate the aquifer-stream interaction. Within the RIV package, the river stage (HRIV) and the river bottom (RBOT) are assigned constant and positive such that the riverbed stays saturated. The riverbed conductance (CRIV) is calculated for each river reach by using the river width in that specific reach and the thickness of the streambed is assumed as half of the vertical dimension of the finite-difference cell (i.e. half of aquifer thickness). In the literature, several methods are suggested to define the streambed conductance (Mehl and

Hill, 2010, Pauw et al., 2015, Harbaugh, 2005). In this case, no clogging layer is assigned underneath the streambed as in Anderson (2005), Mehl and Hill (2010), and Morel-Seytoux et al. (2014), and the river is not penetrating (i.e. it is located on top of the aquifer). Therefore, we consider the head losses occurring from the bottom of the stream to the finite-difference node in the centre of the aquifer. This is equal to equation (4) of Mehl and Hill (2010) where the streambed and the aquifer hydraulic conductivities are the same, and calculated as follows:

$$C^* = \frac{KD}{0.5H} \quad (4)$$

Due to the large number of simulations, MODFLOW is piloted from a MATLAB script using the mflab package (Olsthoorn, 2013). The Preconditioned Conjugate-Gradient (PCG) package is utilised as the mathematical solver in this study with convergence criteria for head change (HCLOSE) set to 0.0001 [L] and the residual criterion for convergence (RCLOSE) set to 0.0001 [L³/T]. The maximum inner iterations and maximum outer iteration was set to 200. The matrix conditioning method was chosen as Modified Incomplete Cholesky.

2.3. Three-cell Model Solution

An analytical expression is developed for the numerical solution of the three-cell model of **Error! Reference source not found.** The overall mass balance equation for the model domain gives:

$$Q_l = Q_r + Q_{riv} \quad (5)$$

Where Q_l and Q_r are the regional fluxes at left and right of the model domain. It should be noted that a linear variation in flux is assumed due to the aquifer being confined, and as such, the regional fluxes are assumed constant up to the interface of the river cell boundary. Using Darcy's law, Q_r and Q_l are imposed as:

$$Q_r = -KH \frac{h_r - h_i}{dx} \quad (6)$$

$$Q_l = -KH \frac{h_i - h_l}{dx} \quad (7)$$

Where h_r and h_l are heads at the centre of the right and left cells and h_i is the head at the centre of the river cell. The Cauchy or head-dependent boundary employed to produce the exchange flow between the river reach and the underlying cell (Harbaugh, 2005) is given as:

$$QRIV = -C^*(h^* - h_i) \quad (8)$$

Replacing the head dependent boundary of equation (8) in the overall mass balance of equation (5) gives:

$$Ql - Qr = -KD \frac{h^* - h_i}{0.5H} \quad (9)$$

Solving the equation (6) for h_i gives:

$$h_i = \frac{Qr * dx}{KH} + h_r \quad (10)$$

Replacing equation (10) in (9) and solving for h_r gives an expression to calculate the head in the right cell of the model.

$$(h_r)_{Numerical} = -\frac{Qr * dx}{KH} + \frac{QlH}{2KD} - \frac{QrH}{2KD} + h^* \quad (11)$$

Similarities and differences can be identified between the analytical solution of equation (1) and the numerical solution of equation (11). The first term in both equations represents the influence of the horizontal component of the flow between the river and the point where the head is evaluated. The second and third terms in both equations account for the effect of vertical head loss within the aquifer. The difference between the two is that a linear relationship assumed between head losses and vertical flow in the numerical solution. Another significant source of difference is that equation (1) is a function of river location (b) (embedded in L), whereas equation (4), and subsequently equation (11) operate independent of b .

2.4. Error Definition

The errors induced to the numerical model from the effects of horizontal discretization and the river position are studied by calculating the heads at the right of the model domain and comparing it with the hydraulic head calculated from the exact solution. Firstly, the head values at the far distance ($L = 2H$) away from the left edge of the river (h_l), and river stage (h^*) are imposed such that the river and aquifer stay connected at all times. Secondly, inserting the imposed values in equation (2), and having the Q_r/Q_l ratios, values of Q_l and Q_r are calculated individually at the distance $L = 2H$. Thirdly, values of Q_r and Q_l are replaced in equation 1 to calculate $(h_r)_{Exact-Analytical}$, and in the numerical model to produce $(h_r)_{Numerical}$ at the distance of evaluation. The difference between the two is finally normalized by $(h_l - h^*)_{Exact-Analytical}$, which is a measure of total head variations throughout the model and always remain positive and constant. This gives the error ε [%] as:

$$\varepsilon(\%) = \frac{(h_r)_{Numerical} - (h_r)_{Exact-Analytical}}{(h_l - h^*)_{Exact-Analytical}} * 100 \quad (12)$$

In the case of the three-cell model, equation (12) can be expanded by making use of equations (1), (2) and (11), thus giving:

$$\varepsilon(\%) = \frac{\frac{(Q_l - Q_r)H}{2KD} + \frac{Q_r(L - dx)}{KH} - \frac{Q_r}{K\pi} \ln\left(\frac{1 - \gamma^{0.5}}{1 + \gamma^{0.5}}\right) + \frac{Q_l}{K\pi} \ln\left(\frac{1}{4}(1 - \gamma)\right)}{(h_l - h^*)_{Exact-Analytical}} \quad (13)$$

Equation (13) is only valid to calculate the error from the limited case of the three-cell model (**Error! Reference source not found.**). In order to calculate the error for other arrangements (**Error! Reference source not found.** and Figure 5), MODFLOW 2005 (Harbaugh, 2005) is utilised to obtain $(h_r)_{numerical}$ for equation (12). As previously mentioned, in such situations, multiple cells on the right and left of the river may be created in the numerical model, such that the far distance condition is satisfied. In the general case, the number of river cells and total cells may vary according to the horizontal discretization step, river geometry and the far distance. Thus, depending on the ratio of horizontal discretization to the river width (dx/D), hereinafter cell to river ratio, the river may occupy numerous cells as in **Error! Reference source**

not found., only part of a large cell as in **Error! Reference source not found.**, or a few cells as in Figure 5. In all cases, the river may overlay some cells only partly.

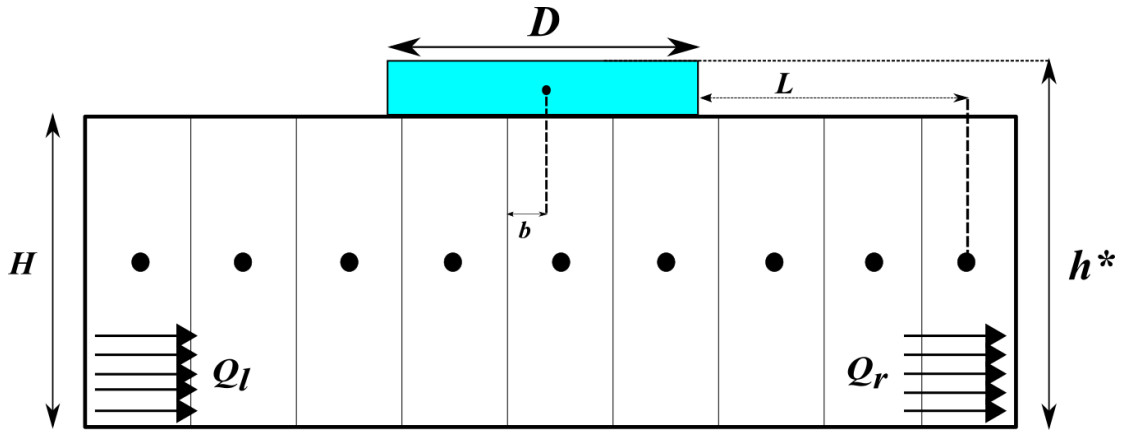


Figure 5. Schematic representation of the numerical setting when the river occupies some river cells fully while other partly.

Anderson (2005) determined the heads under a Dupuit assumption using a continuous solution along the x-axis as equation (14).

$$(h_r)_{Dupuit} = -\frac{Q_r}{KH} + \frac{Q_l}{\sqrt{2} K \sin\left(\frac{D}{H\sqrt{0.5}}\right)} - \frac{Q_r \coth\left(\frac{D}{H\sqrt{0.5}}\right)}{\sqrt{2} K} + h^* \quad (14)$$

This solution can be viewed as a limited case of our numerical setting where extremely fine horizontal discretization employed underneath the stream (i.e. when $dx \rightarrow 0$). The errors from this situation are thus defined as the difference between equation (14) and the exact solution given in equation (1):

$$\varepsilon(\%) = \frac{(h_r)_{Dupuit} - (h_r)_{Exact}}{(h_l - h^*)_{Exact}} \quad (15)$$

Equation (15) can be expanded as follows.

$$\varepsilon(\%) = \frac{\frac{Q_r \pi \coth\left(\frac{D}{H\sqrt{0.5}}\right)}{\sqrt{2} Q_l} + \frac{\pi \operatorname{csch}\left(\frac{D}{H\sqrt{0.5}}\right)}{\sqrt{2}} + \ln\left(\frac{1-\gamma^{0.5}}{1+\gamma^{0.5}}\right) - \left(\frac{Q_r}{Q_l}\right) \ln\left(\frac{1}{4}(1-\gamma)\right)}{\frac{L\pi}{H} + \left(\frac{Q_r}{Q_l}\right) \ln\left(\frac{1-\gamma^{0.5}}{1+\gamma^{0.5}}\right) - \ln\left(\frac{1}{4}(1-\gamma)\right)} \quad (16)$$

Equation (16) shows that the errors generated in the model by adopting the Dupuit assumption (or $dx \rightarrow 0$) are only a function of the river channel geometry (D/H) and flow conditions (Q_r/Q_l) (Anderson, 2005). However, in the numerical context (Eq. 13), the error depends not only on these two parameters, but also on the horizontal grid spacing (dx) and the position of the river within the river cell (b , embedded in L).

2.5. Equivalent Parameter

As previously mentioned, the single parameter used for simulating the groundwater-surface water exchange (the conductance) is classically treated as an equivalent parameter and adjusted through the calibration process. To assess the suitability of this approach, Anderson (2005) previously treated the streambed vertical resistance (basically the inverse of conductance) as an equivalent parameter in the 1D continuous Dupuit model and evaluated the dependence of this parameter on river geometry and flow conditions. Figure 4 of Anderson (2005) demonstrates that the equivalent parameter varies significantly with river geometry (D/H) and flow conditions (Q_r/Q_l), especially for narrow streams. Here, a similar strategy is employed to investigate the efficiency of the streambed conductance as an equivalent parameter in the numerical context for the case of the three-cell model. We equate the head values from the numerical solution (Eq. 11) to the exact values from the analytic solution (Eq. 1), and solve for equivalent conductance C_{eq} [L/T]. This gives:

$$C_{eq} = \frac{1 - \frac{Q_r}{Q_l}}{\frac{Q_r}{Q_l} \frac{(dx - L)}{KH} + \frac{Q_r}{Q_l} \frac{1}{K\pi} \ln\left(\frac{1}{4}(1 - \gamma)\right) - \frac{1}{K\pi} \ln\left(\frac{1 - \gamma^{0.5}}{1 + \gamma^{0.5}}\right)} \quad (17)$$

Equation (17) shows that the calibrated parameter is not only a function of physical properties (stream geometry, D/H) but also varies in response to regional flows (Q_r/Q_l), numerical cell dimensions (dx), and also position of the river in the numerical cell (b) (embedded in L).

3. Results

We impose the head at the left boundary of the study area (h_l) and maintain the river stage (h^*) to a constant positive value to always maintain the river and aquifer hydraulically connected. The flow conditions are then varied in the range of $-1 \leq Q_r/Q_l \leq 1$, and the head on the right side of the domain (h_r) is evaluated. The Q_r/Q_l values between -1 and 1 covers the entire range of flow conditions and values outside of this boundary are considered by assuming the symmetry of the problem. For instance, the solution for $Q_r/Q_l = 5$ is alike $Q_r/Q_l = 1/5$ if the right and left of the problem is inverted (Anderson, 2005). It should be noted that if Q_r/Q_l outside the range of -1 to 1 needs to be simulated, $(h_l - h^*)_{\text{Exact-Analytical}}$ may not be the measure of total head variation in the problem domain and needs to be modified.

3.1. Effects of Horizontal Discretization

The errors introduced in the numerical model due to horizontal discretization are calculated using Equation (12) and are summarized in Figure 6. In several sets of simulations, the river geometry (D/H), river location (b) and flow fields (Q_r/Q_l) are maintained as constant values, and the horizontal discretization altered by changing dx/D . The results of this section have been achieved for a case of river being located in the centre of the model domain at all times ($b/dx=0.5$). Three flow conditions are studied: $Q_r/Q_l = 1$, $Q_r/Q_l = 0$ and $Q_r/Q_l = -1$, which depict the extremes of flow condition as explained in section 2.2 and all the other possible flow regimes lie between them. The results provided for three different stream geometries (D/H) to investigate the sensitivity of error to proportional width of the stream. Three different river geometries are selected with five-fold increases as $D/H = 0.2$, $D/H = 1$ and $D/H = 5$.

Proportion of the horizontal width of the cell to the river width is indicated by using the parameter dx/D . $dx/D < 1$, represents a condition in which the whole width of the river is modelled by using multiple cells (**Error! Reference source not found.** and Figure 5), $dx/D > 1$ represent situations where the river is being modelled via a single river cell (**Error! Reference source not found.**), and $dx/D = 1$ models a single cell width of which is fully occupied by the river. The result presented in this section comprises a range of

dx/D values starting from extremely small value of $dx/D=0.001$ to $dx/D=1$. The error values for dx/D values greater than one are equal to $dx/D=1$, and as such they are not included in the graphs of Figure 6 **Error! Reference source not found.**. To have an extensive and continuous analysis of effects of horizontal discretization, dx/D values are risen with small steps of 0.001. The smallest dx/D in each graph of Figure 6 shows a situation where the horizontal grid spacing is extremely fine, able to reproduce identical results as the continuous analytical solution, given by Equation (16). Therefore, the error values at the beginning of each graph are only consequence of the vertical coarsening of the model by using a single layer model, and should not be accounted for horizontal discretization.

Figure 6.a depicts the error for the smallest channel geometry ($D/H=0.2$). By changing the dx/D values, the number of river cells varies from a maximum of 1000 at $dx/D=0.001$ to one cell for $dx/D \geq 1$. For $Q_r/Q_l=1$, the initial value of the error (error of vertical coarsening) is 0.3% and increase in the dx/D values has no effect on changing the value of error. For $Q_r/Q_l=0$ the error of vertical discretization is greater than $Q_r/Q_l=0$ with 70%, but similarly, increasing the horizontal discretization has little effect on the error value and reaches the maximum of 71% at $dx/D=1$. Similar trends but in greater error values observed for $Q_r/Q_l=-1$. Using a single layer model creates an error value of 115% which increases marginally to 117% when $dx/D=1$. It should be noted that the analytical expression of Equation (13) is only valid for a three-cell setting, which in case of $D/H=0.2$, is only valid to calculate the error for values of dx/D greater than 10.5.

Results for $D/H=1$ are shown in Figure 6.b. The number of river cells varies from 1000 cells at $dx/D=0.001$ to one cell for all values of $dx/D \geq 1$. When $Q_r/Q_l=1$, error of vertical discretization is -5%, and coarsening the horizontal grid increases the error values up to 8% for $dx/D \geq 1$. The impact of increasing the horizontal discretization and vertical discretization is slightly greater for this stream geometry, compared to $D/H=0.2$. For $Q_r/Q_l=0$, the error of horizontal discretization drops from 70% at $D/H=0.2$ to 9.5% for the wider river of $D/H=1$. Enlarging the horizontal grid, creates error values up to 5.5% and produces 15% total error at $dx/D \geq 1$. For $Q_r/Q_l=-1$, similar to $Q_r/Q_l=0$, error of horizontal coarsening drops significantly from 115% for $D/H=0.2$ to 22% for the wider river of $D/H=1$. Increasing the dx/D produces error values up to 13% and results in the total error of 35% for $dx/D \geq 1$. The three-cell scenario and applicability of Equation (13) for this arrangement starts at dx/D values greater than 2.5.

The results of the largest channel geometry, $D/H=5$ is illustrated in Figure 6.c. In the finest resolution 1000 river cells simulate the exchange for this geometry and one river cell represents all dx/D values greater than one. The influence of horizontal discretization is more evident for this stream geometry and becomes more dominant in larger values of dx/D . For $Q_r/Q_l=1$, coarsening the model in vertical direction produces error value of -11% which increases with an oscillatory behaviour by coarsening the horizontal grid to the maximum of 84% for dx/D values greater than or equal to one. Vertical discretization produces no error of 0.04% for $Q_r/Q_l=0$, which remains steady by increasing the horizontal discretization up to $dx/D=0.9$. Total error reaches the maximum of 4% for $dx/D \geq 1$. Error trends for $Q_r/Q_l=-1$ is very similar to the $Q_r/Q_l=1$, but with the opposite sign. Error of vertical discretization is 11%, and enlarging the horizontal discretization increase the error values to the maximum of 92% for the dx/D values greater than and equal to one. The three-cell arrangement for this stream geometry is applicable to dx/D values greater than one.

Maximum errors occur when river width occupies the whole area of the river cell (i.e. where the right edge of the river aligns on the right border of the river cell). At this point, the analytical solution calculates the head from the edge of the river to distance L ($L=dx/2$ at this arrangement), while the numerical solution calculates the head from the centre of the river to the centre of the right cell (dx). Due to this distance difference, the numerical solution misrepresents the vertical flow lines compared to the exact analytical solution.

The effect of river geometry (D/H) is studied and comparison between the three graphs of Figure 6 shows a direct correlation between the river geometry and errors induced to the model by horizontal discretization. In $D/H=0.2$ changing the horizontal spacing has little impact on the error value and the errors are dominated by the errors of vertical discretization. At $D/H=1$, the errors from horizontal and vertical discretization are in the same order. For $D/H=5$, conversely, vertical discretization produces 11% error into the model, while the total errors are dominated by the errors induced by the horizontal discretization.

For all cases, the absolute value of the errors for negative Q_r/Q_l values is larger than the other flow conditions. Negative values of Q_r/Q_l represent a condition whereby flux from the right side of the model domain contribute to a converging flow toward the stream, which intensifies the vertical gradients.

Therefore, using the Dupuit approximation induce greater error values for this flow condition. The flow condition of $Q_r/Q_l = 0$ represent a situation that there is no flow from the right of the stream and all the left-side flow is directed towards the stream, creating vertical gradients. As such, errors due to neglecting the vertical flow is also large for this condition. Conversely, $Q_r/Q_l = 1$ represents a throughflow condition which has no contribution to the stream, and the error due to neglecting the vertical flow is zero (Figure 6.a). By increasing the size of the stream, the errors from horizontal discretization controls the error values and the errors induced to the model from vertical coarsening becomes less visible (Figure 6.c)

In Figure 6.b and Figure 6.c, when decreasing the values of dx/D , the error values converge with an oscillating behaviour towards a point where the errors from horizontal discretization becomes insignificant. At $D/H = 1$, errors from horizontal discretization are less than 2% for all values of $dx/D < 0.5$, showing that horizontal refinement more than that point only changes the error by 2%. For $D/H = 5$, error values are less than 2% for all values of $dx/D < 0.11$, indicating that discretizing the river with more than 9 river cells, may only increase the accuracy by 2%. The results from Figure 6.c show that even discretising the river into two smaller cells can reduce the errors by 67%.

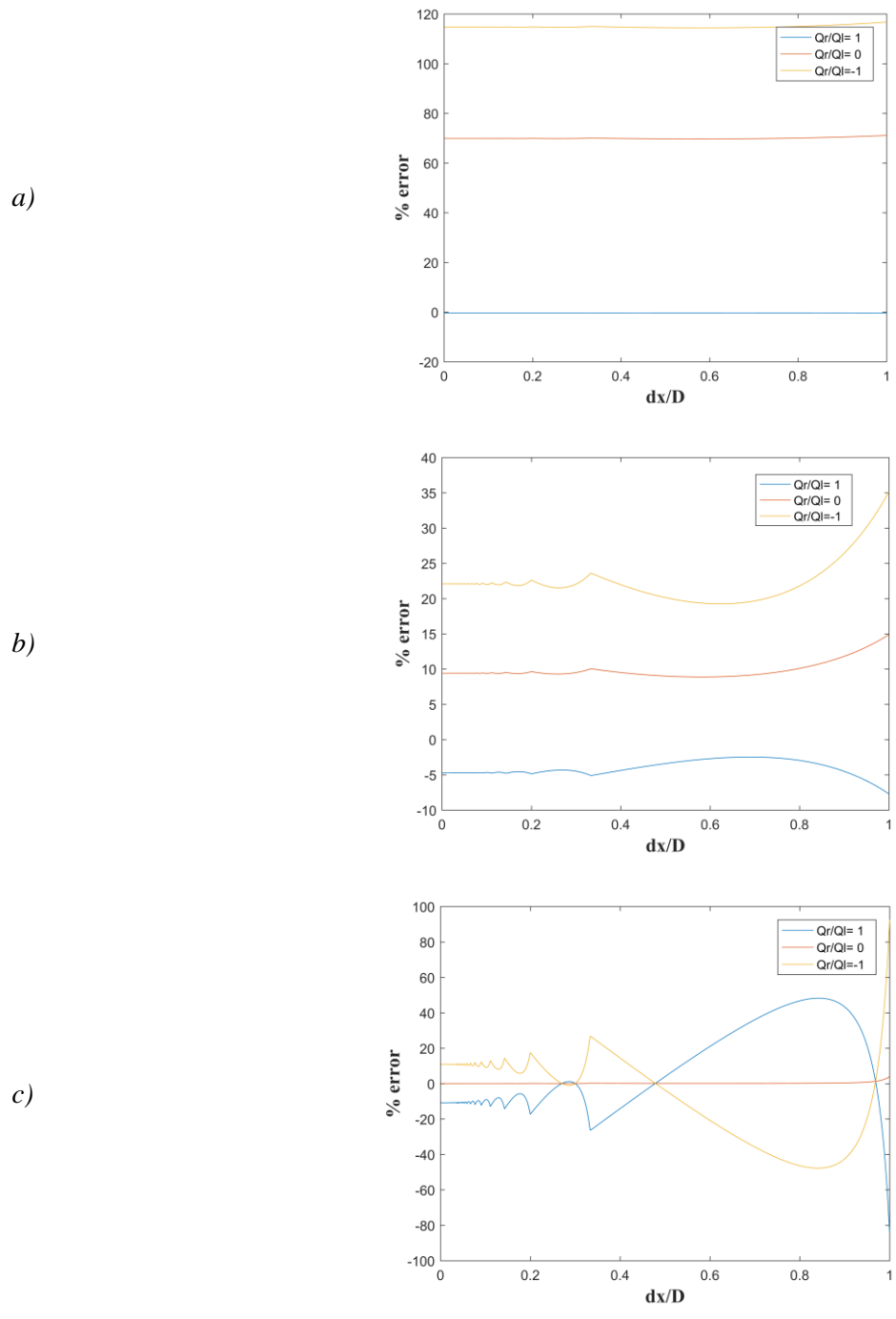


Figure 6. Variations in error in response to horizontal discretization for different river geometries a) $D/H=0.2$; b) $D/H=1$; c) $D/H=5$

3.2. Effect of River Position

The influence of stream position (b/dx) within the numerical cell is studied and the results are collated in Figure 7. Similar to the last section, the comparison is made for three river geometries (D/H) which are selected with five-fold increases as $D/H = 0.2$, $D/H = 1$ and $D/H = 5$. For each river geometry, effects of river position are studied by considering five different horizontal discretization as $dx/D = 0.1$, $dx/D = 0.5$, $dx/D = 1$, $dx/D = 5$ and $dx/D = 10$. As depicted in Figure 7, results for each river geometry presented in a specific row, and dx/D values shown in a separate column. Similar to section 3.1, the results are investigated for three different flow regimes as $Q_r/Q_l = 1$, $Q_r/Q_l = 0$ and $Q_r/Q_l = -1$, which are indicated in three lines with distinctive colours. In each simulation, the values of dx/D and D/H are constant and the position of river is altered by changing b/dx between 0 and 1. For consistency with section 3.1, the error values indicated in Figure 7 are inclusive of errors induced to the model by vertical and horizontal discretization and the term *total error* is used for them. However, since the results of section 3.1 achieved for a limit case of a river being located in the centre of the domain (i.e. $b/dx = 0.5$), the errors for different b/dx values are reported in the text of this section as the deviation from the error at $b/dx = 0.5$.

The results for the smallest river geometry, $D/H = 0.2$, are shown in Figure 7.1. As shown in Figures 7.1.a and 7.1.b no response has been observed as a result of variations of b/dx and as mentioned, the indicated values are the initial values induced by vertical discretization. Marginal changes appear in Figure 7.1.c by changing the river position towards $b/dx = 0$ and $b/dx = 1$. The error values deviate up to 3% for $Q_r/Q_l = -1$ and up to 2% for $Q_r/Q_l = 0$ from the situation that the river is in the centre. The sensitivity to b/dx becomes more evident by increasing the width of the cell as shown in Figure 7.1.d. In this arrangement, river positions in the range of $0.1 \leq b/dx \leq 0.9$ simulate an arrangement that the river is located within the boundaries of one cell, while at $b/dx < 0.1$ and $b/dx > 0.9$, a portion of the river is located in a second river cell. For $Q_r/Q_l = 1$, maximum error of 19% occur twice at $b/dx = 0.9$ and $b/dx = 0.1$, but changes sign and decrease down to 2% for cases when two cells represent the stream. For $Q_r/Q_l = 0$, moving the river along the extent of one cell has no effect on the error value, but the errors increase up to 8% when $b/dx < 0.1$ and $b/dx > 0.9$. For $Q_r/Q_l = -1$, the error has an increasing trend when the river is shifting farther from the centre in the range of $0.1 \leq b/dx \leq 0.9$, and keep increasing to a maximum of 15% when $b/dx = 0$ and $b/dx = 1$. An increase in error values observed when the horizontal

discretization is increased to $dx/D=10$ as shown in Figure 7.1.e. At this arrangement, river positions in the range of $0.05 \leq b/dx \leq 0.95$ are modelled with a single river cell, but the number of river cells changes to two for the b/dx values outside of this range. For $Q_r/Q_l = 1$, the error values are at their maximums occurring twice at $b/dx = 0.05$ and $b/dx = 0.95$ with 43% greater than the situation where river is in the centre, but change trend at $b/dx < 0.05$ and $b/dx > 0.95$ and decline rapidly to errors of the $b/dx = 0.5$. For $Q_r/Q_l = 0$, the errors are constant on the range of $0.05 \leq b/dx \leq 0.95$, but varies up to 16% at conditions that two cells represent the river. For $Q_r/Q_l = -1$, shifting the river position away from the centre of the cell increases the quantity of error by the maximum of 36% at $b/dx = 0.02$, and a change in error trend occur at $b/dx = 0.95$ which two cells simulate the river.

The effect of river position for the larger stream geometry of $D/H = 1$ is presented in Figure 7.2. As shown in Figure 7.2.a, altering the b/dx values induces no error in the smallest value of dx/D . At $dx/D = 0.5$, variations of b/dx marginally changes the error values up to 2% for $Q_r/Q_l = 1$ and $Q_r/Q_l = 0$, and up to 5% for $Q_r/Q_l = -1$. Figure 7.2.c simulate a situation that river and cell width are in the same size, but apart from $b/dx = 0.5$, all the values of b/dx simulate the river by using two cells. For flow conditions of $Q_r/Q_l = 1$ and $Q_r/Q_l = 0$, altering the value of b/dx changes the error values up to 9% from the error value at the arrangement of $b/dx = 0.5$. For $Q_r/Q_l = -1$, shifting the river away from the centre of the domain induces error values up to 20% at $b/dx = 0$ and $b/dx = 1$. Influence of river position becomes more apparent in larger horizontal discretization. In Figure 7.2.d, position of river in the range of $0.1 \leq b/dx \leq 0.9$, represent a situation which river is only modelled by one cell, but b/dx values outside of this range are using two river cells to simulate the arrangement. For $Q_r/Q_l = 1$ and $Q_r/Q_l = -1$, the error values are gradually increasing by moving the river away from the centre of the cell in the range of $0.1 \leq b/dx \leq 0.9$ and reaches the maximum difference of 86% for $Q_r/Q_l = 1$ and 77% for $Q_r/Q_l = -1$, occurring twice at $b/dx = 0.9$ and $b/dx = 0.1$. For both $Q_r/Q_l = 1$ and $Q_r/Q_l = -1$, values of $b/dx > 0.9$, at which the number of river cells increases to two, a change in the trend of the error is noticeable. For flow condition of $Q_r/Q_l = 0$, moving the river within one cell has no effect on the error value but at $b/dx < 0.1$ and $b/dx > 0.9$ where two river cells simulate the river, maximum of 15% decline observed. Similar trends observed for the largest horizontal discretization, but in greater values. For $dx/D = 10$, river positions in the range of $0.05 \leq b/dx \leq 0.95$ are simulated by using only one river cell, while b/dx values

outside this range are modelled by utilizing two river cells. For $Q_r/Q_l=1$ and $Q_r/Q_l=-1$, a steady increase observed in the error values when the river gets farther from the centre of the cell such that changes the value of error by 194% and 174%, respectively, $b/dx = 0.05$ and $b/dx = 0.95$ (occur twice). For both flow condition, error values change sign and start decreasing for b/dx values greater than 0.95. For $Q_r/Q_l=0$, position of the river has no effect in the range of $0.05 \leq b/dx \leq 0.95$, but outside this boundary, up to 17% error difference observed.

Effects of the river position on the widest stream geometry, $D/H = 5$, are shown in Figure 7.3.a to Figure 7.3.e. Variations of b/dx has minor effects on the smallest horizontal discretization as shown in Figure 7.3.a. Minor changes has been observed for $Q_r/Q_l=1$ and $Q_r/Q_l=-1$ with changes up to 3%, occurring twice at $b/dx = 0$ and $b/dx = 1$. Variations of b/dx has no effect on the error values of $Q_r/Q_l=0$. For $dx/D = 0.5$, the errors are at their minimum when $b/dx = 0.5$. For $Q_r/Q_l=1$ and $Q_r/Q_l=-1$, altering b/dx changes the errors up to 45% occurring at $b/dx = 0$ and $b/dx = 1$. No change observed when varying the b/dx values for the flow condition of $Q_r/Q_l=0$. For $dx/D = 1$, apart from $b/dx = 0.5$, the entire range of b/dx values simulate the exchange by using two river cells. By moving the stream towards $b/dx = 0$ and $b/dx = 1$, error gradually varies up to 95%, 4% and 102% for $Q_r/Q_l=1$, $Q_r/Q_l=0$ and $Q_r/Q_l=-1$, respectively. It is noticeable that error values produce a linear trend in $b/dx < 0.5$, while a curvilinear behaviour is observed for $b/dx > 0.5$. For $dx/D = 5$, river position in the range of $0.1 \leq b/dx \leq 0.9$ simulated by using only one numerical cell, but two river cells used outside for b/dx values outside this range. For $Q_r/Q_l=1$ and $Q_r/Q_l=-1$, error values are linearly increasing by moving the river away from the centre of the cell, such that it changes by the maximum of 557% for $Q_r/Q_l=1$ and 565% for $Q_r/Q_l=-1$ when the position of river is at $b/dx = 0.93$. For both flow regimes, the error change sign for b/dx values greater than 0.9. For $Q_r/Q_l=0$, the error shows no sensitivity when the position of river changes on the extent of one cell, but 4% error induces to the model at $b/dx < 0.1$, and $b/dx > 0.9$. Similar trends, but in greater error values observed for the largest horizontal discretization, $dx/D = 10$. In this situation, river positions in the range of $0.05 \leq b/dx \leq 0.95$, modelled by using one river cell, while two river cells utilised for outside this boundary. For $Q_r/Q_l=1$ and $Q_r/Q_l=-1$, a linear error trend observed when shifting the error away from the centre of the cell, reaching the maximum difference of 1066% and 1073%, respectively, occurring at $b/dx \leq 0.96$. At $b/dx \leq 0.95$, the error values change sign

and start decreasing. For $Q_r/Q_l=0$, the error is constant in the range of $0.05 \leq b/dx \leq 0.95$, but a 4% error induces to the model for b/dx values outside this range.

Figure 7.1.a to 7.1.e show that when the stream is narrow, location of the river introduce little, if any, error into the model. These errors, at their maximum, introduce 35% percent discrepancy when the cell width is ten times larger than the river width and the river is attached to the borders of the river cell(s). For the wider river geometry ($D/H=1$), the position of the river has more influence on the error values, such that at $dx/D=10$, when the cell width is ten times larger than river width, errors up to 195% induce to the model domain. For this river geometry, the effects of river location are less than 20% for dx/D values smaller than one. The effects of river position are at their maximum for the widest river geometry $D/H=5$, creating enormous errors up to 1074% when the cell width is ten times larger than the river width and the river is adjacent to the border of the river cell. For this river, the effects of b/dx are minor (up to 3%) for $dx/D=0.1$.

The total errors (i.e. the error from vertical coarsening, horizontal coarsening and location of the river as shown in Figure 7) reaches to their maximum values when the edges of the river align with the borders of the river. This situation occurs at $b/dx=0.5$ when $dx/D=1$, at $b/dx=0.1$ and 0.9 when $dx/D=5$ and $b/dx=0.05$ and 0.95 when $dx/D=10$. At this situation, the numerical solution is unable to capture the vertical gradients occurring outside the physical boundaries of the river cell, creating a large discrepancy between the numerical and the analytical solutions to represent the flowlines.

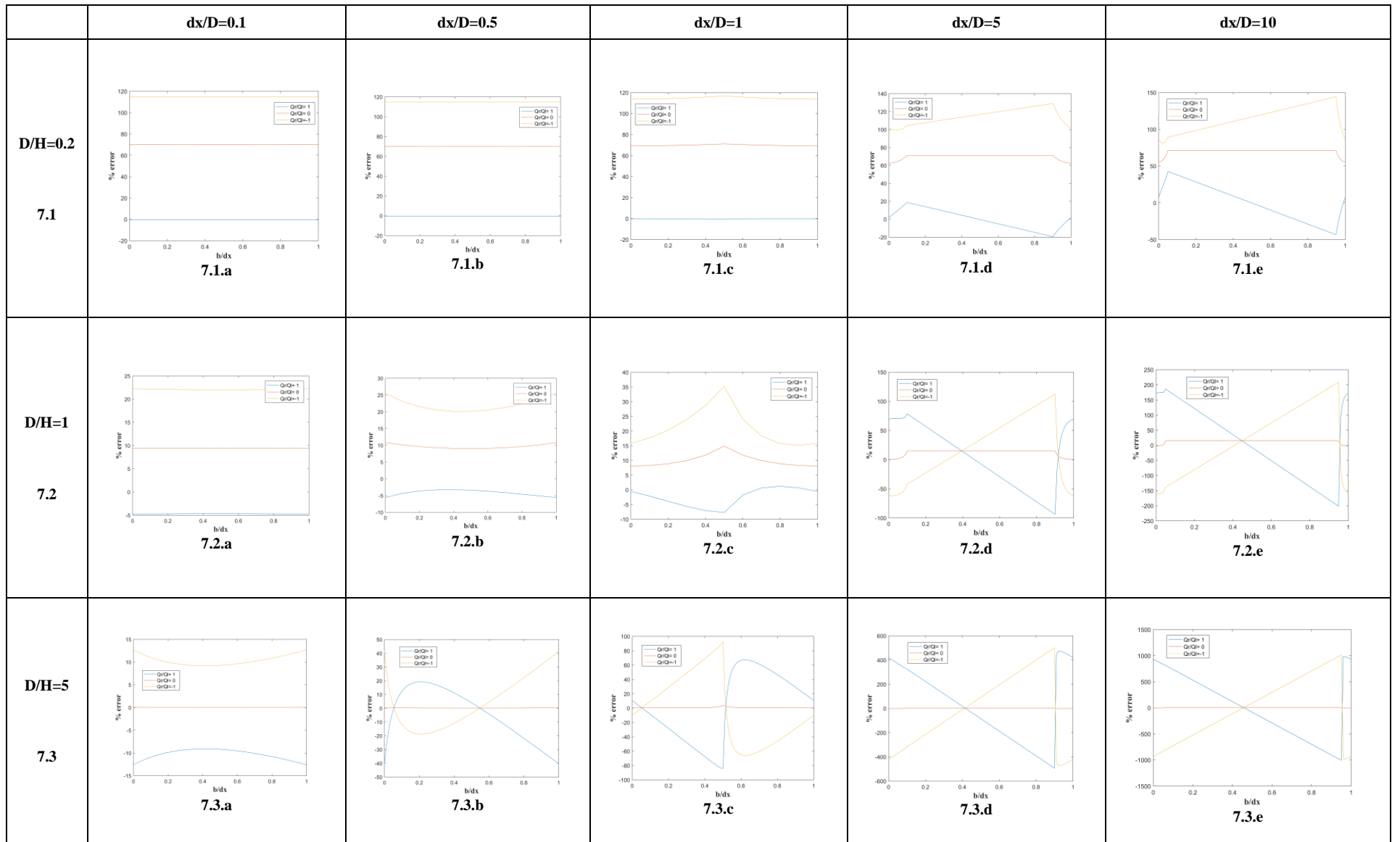


Figure 7. Error variation in response to the location of the river in the numerical cell

In all arrangements, errors induced by the position of the river shown similar trends and magnitudes for $Q_r/Q_l = 1$ and $Q_r/Q_l = -1$, but with total error values due to different effects from vertical discretization. Errors for $Q_r/Q_l = 0$ changed little compared to the other flow regimes, since the term containing the river position is cancelled from equation (13) for this flow condition.

When the horizontal discretization is large (e.g. $dx/D = 5$ and $dx/D = 10$), the total error value reaches zero at a certain b/dx values. In the context of the three-cell model, an expression developed from the equation (13) to calculate the position of this point as follows:

$$\frac{b'}{dx} = \frac{1}{2} \left(\frac{H}{D} \right) \left(\frac{H}{dx} \right) \left(\frac{Q_r}{Q_l} - 1 \right) + \frac{H}{dx} \left(\frac{Q_r}{Q_l} - \frac{\ln \left(\frac{1}{4} (1 - \gamma) \right)}{\pi} \right) - \frac{1}{2} \frac{D}{dx} - \frac{Q_r}{Q_l} - 1.5 \quad (18)$$

Where b'/dx is the river position in which the error between the numerical solution (Eq. 11) and the exact solution (Eq. 1) is zero. This point can vary as a function of river geometry (D/H), cell to river ratio (dx/D) and flow conditions (Q_r/Q_l).

3.3. Equivalent parameter and the river geometry

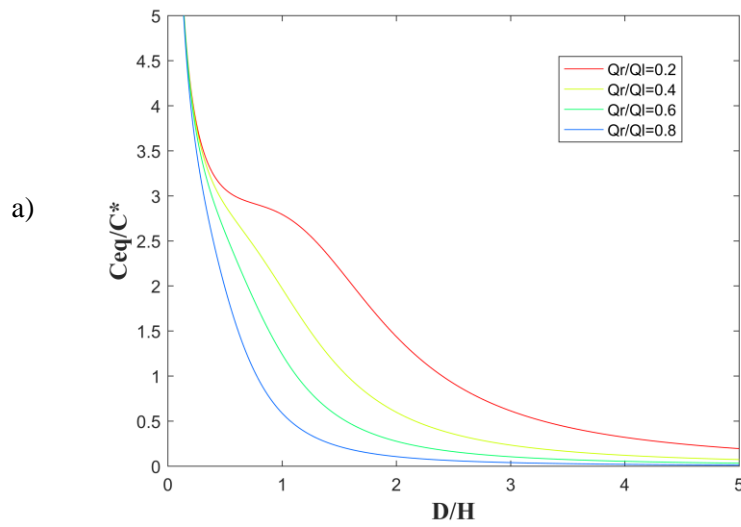
The capacity of the clogging layer conceptualisation, as a single calibrating parameter, to efficiently calculate the GW-SW exchange is evaluated in this section. The values of the equivalent parameter (Eq. 17), achieved through calibrating the numerical model by the exact solution and solving for the equivalent conductance (C_{eq}). The equivalent conductance is normalized by the theoretical conductance (Eq. 4) to produce a dimensionless parameter (C_{eq}/C^*) called *dimensionless conductance*. In this section, effects of river geometry (D/H) and flow conditions (Q_r/Q_l) on dimensionless conductance investigated and the results are summarised in Figure 8. It should be noted that since the equation (17) is derived for the limit case of the three-cell model (**Error! Reference source not found.**) the results of this section are only applicable in that context.

Similar to section 3.1, results of this section are reported for the particular case of the river being in the centre of the cell ($b/dx = 0.5$). The river geometries studied are in the range of $0.01 \leq D/H \leq 5$ which

is inclusive of the geometries studied in previous sections. For the small river geometries to be included in the context of the three-cell model, a very large dx/D value should be assigned, such that the far distance condition could be met. As such the cell to river ratio was assigned as $dx/D = 400$. It should be noted that when river is in the centre of the cell ($b/dx = 0.5$), the results are independent of the horizontal discretization. Similar to previous sections, flow conditions are considered in the range of $-1 \leq Q_r/Q_l \leq 1$, but 0.2 steps are selected for a finer representation of the sensitivity of equivalent conductance on flow conditions. Due to distinct responses to flow conditions, results are presented separately for $Q_r/Q_l > 0$ and $Q_r/Q_l \leq 0$ as in Figure 8a and Figure 8b.

In Figure 8a, four lines are depicted, showing results for $Q_r/Q_l = 0.2$, $Q_r/Q_l = 0.4$, $Q_r/Q_l = 0.6$, and $Q_r/Q_l = 0.8$. Equivalent conductance for $Q_r/Q_l = 1$ is not shown in Figure 8a as the equation (17) becomes zero for all situations of this flow condition. Values of the equivalent conductance (C_{eq}) are very different from the theoretical conductance (C^*) when the river geometry is either very small or very large. Maximum value of C_{eq}/C^* occurs at $D/H = 0.01$, with the converged value of 32.4 for all flow conditions (not shown in Figure 8a). The C_{eq}/C^* values decline rapidly such that at $D/H = 0.2$ calculated between 4 and 4.2 for different flow conditions. At $D/H = 1$, the dimensionless conductance is more sensitive to flow condition and calculated between 0.6 and 2.8. Dimensionless conductance for all flow conditions decreases to values smaller than one for stream geometries (D/H) greater than 2.4. At $D/H = 5$, dimensionless conductance is calculated as 0.19, 0.07, 0.03 and 0.1 for $Q_r/Q_l = 0.2$ to $Q_r/Q_l = 0.8$, respectively. Figure 8a show that larger values of Q_r/Q_l have a greater influence on C_{eq}/C^* when altering the values of D/H .

$$Q_r/Q_l > 0$$



$$Q_r/Q_l \leq 0$$

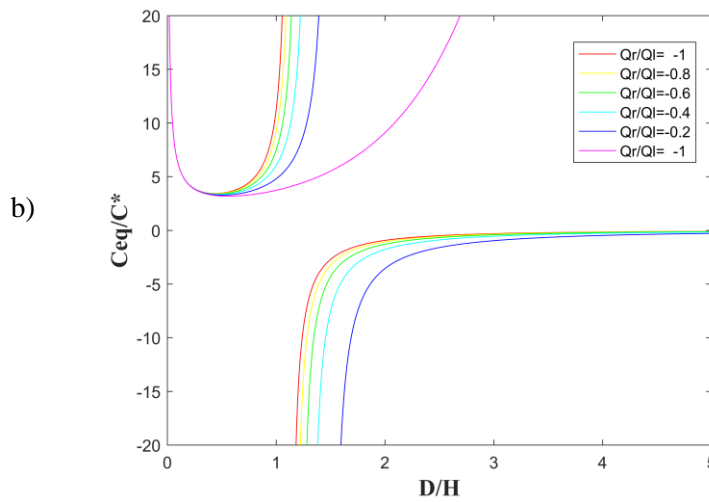


Figure 8. Streambed conductance as an equivalent parameter in the three-cell context for $b/dx=0.5$

In Figure 8b, six lines show the variations for different flow conditions as $Q_r/Q_l = 0$, $Q_r/Q_l = -0.2$, $Q_r/Q_l = -0.4$, $Q_r/Q_l = -0.6$, $Q_r/Q_l = -0.8$, and $Q_r/Q_l = -1$. Apart from $Q_r/Q_l = 0$, a discontinuity appear for all flow conditions, occurring between $D/H = 1.1$ and $D/H = 1.5$. Similar to positive Q_r/Q_l values, maximum value of dimensionless conductance occurs at the smallest stream geometry, $D/H = 0.01$ with 32.4. For rivers geometries up to $D/H = 0.3$, flow condition has insignificant effects

such that C_{eq}/C^* calculated 3.6 for all flow conditions. The river location in which the discontinuity appears vary upon the value of Q_r/Q_l , cell to river ratio (dx/D) and river geometry (D/H) and can be calculated as follows:

$$\frac{b^*}{dx} = \frac{Q_l}{Q_r} \frac{H}{dx} \frac{\ln\left(\frac{1-\gamma^{0.5}}{1+\gamma^{0.5}}\right)}{\pi} - \frac{H}{dx} \frac{\ln\left(\frac{1}{4}(1-\gamma)\right)}{\pi} - \frac{1}{2} \frac{D}{dx} + 0.5 \quad (19)$$

Where b^*/dx is the location at which a discontinuity occur the dimensionless conductance. For $Q_r/Q_l=0$, the equation (17) becomes a logarithmic function of D/H and as such the dimensionless conductance is constantly increasing by rising the river geometry, and reaches to 405 (not shown in the graph) for $D/H = 5$.

Figure 4 of Anderson (2005) shows that the value of equivalent parameter tend to increase for wider rivers when an analytical approach is adopted. However, Figure 8 shows that the equivalent conductance (C_{eq}) show a different trend when the river is defined in a numerical cell, as the equivalent parameter tends to decline when the river increase in width and occupies a larger portion of the cell.

3.4. Equivalent parameter and river location

Since the riverbed conductance becomes independent of dx when river is located in the centre of the cell, the sensitivity of the dimensionless conductance (C_{eq}/C^*) in response to variations of b/dx is studied separately in this section. Similar to section 3.1, three river geometries (D/H) considered, with five-fold increases as $D/H=0.2, 1$ and 5 . For each river geometry, two different cell size selected to investigate the the effects of cell size; one selected such that represents the minimum cell-size applicable as three-cell model, and the other selected relatively large as $dx = 20H$. Flow conditions (Q_r/Q_l) are again considered between -1 and 1, with steps of 0.2 (Figure 9).

For most Q_r/Q_l values, a discontinuity is evident in all graphs of Figure 9, the location of which can be calculated using equation (19). It should be noted that the result of this section are achieved by using equation (17) and are only applicable to the context of three-cell model.

In each calculation, the value of dx/D maintained constant, and the position of the stream is adjusted by varying the river position between $D/2$ and $dx - D/2$. These boundary conditions ensure that the river overlies only one cell, and stays in the range of three-cell model. Maintaining the river position at $b = D/2$ simulates an arrangement that the stream edge is aligned to the left border of the numerical cell and at $b = dx - D/2$ the river located precisely on the right end of the river cell. Altering the b/dx within this range then represents the entire possible arrangements of river position.

For the narrowest stream, $D/H=0.2$, one dx/D value selected as 20, which is the minimum value that the three-cell model can be applied and the other is $dx/D=100$ (i.e. $dx = 20H$). When $dx/D=20$ and $Q_r/Q_l > 0$, discontinuities appear when the river is on the left side of the river ($b/dx < 0.5$), while for $Q_r/Q_l < 0$, they happen when the river is located on the right side of the cell space ($b/dx > 0.5$) (Figure 9a). At $dx/D=100$, discontinuities occur in the same sides, but they are more concentrated when the river is adjacent to the centre of the cell. Values of dimensionless conductance are observed to be less dependent on flow conditions where the river is located adjacent to the border of the cell (Figure 9b). For both horizontal discretization, dimensionless conductance for $Q_r/Q_l = 0$ is constantly equal to 4.2 and for $Q_r/Q_l = 1$ always calculated zero.

For $D/H=1$, values of dx/D are selected as 4 and 20. When $dx/D=4$, the discontinuities occur in the range of $0.3 < b/dx < 0.7$ and outside this range the values of dimensionless conductance calculated between -4 to 4 (Figure 9c). For the wider cell ($dx/D=20$), all the range of discontinuities occur between $0.45 < b/dx < 0.55$, and values of dimensionless conductance outside this range marginally varies between -0.4 and 0.4 (Figure 9.d). Dimensionless conductance for flow conditions of $Q_r/Q_l = 0$ and $Q_r/Q_l = 1$, calculated as 3.7 and 0, respectively.

For the widest river ($D/H=5$), $dx/D=1.1$ and $dx/D=4$ are selected. For $dx/D=1.1$, since the width of the river and cell are not very different, values of b/dx range only from 0.45 to 0.55, and as such, no discontinuity appears in the graph. Values of dimensionless conductance vary between 0.25 and 0.35 for different Q_r/Q_l , and vary as little as 0.1 by changing the river location (Figure 9e). For the larger cell sizes ($dx/D=4$), discontinuities of the graphs occur mainly when the river is on the left of the river cell in the range of $0.35 < b/dx < 0.45$. When the river is closer to the borders of the cell, values of dimensionless

conductance calculated between +0.15 and -0.1. Values of dimensionless conductance for $Q_r/Q_l = 0$ is calculated significantly larger as 404 (not shown in graph), and for $Q_r/Q_l = 1$ it is calculated as zero.

Result show that when the stream is farther away from the centre of the cell, the values of dimensionless conductance are in smaller magnitudes. Secondly, when the river is away from the centre of the cell, changes in flow conditions have lesser effects on the values of dimensionless conductance. Those effects, however, can have strong influences when the river is closer to the range of discontinuities. For a constant cell size, rivers of larger geometry, observed to have smaller values of dimensionless conductance.

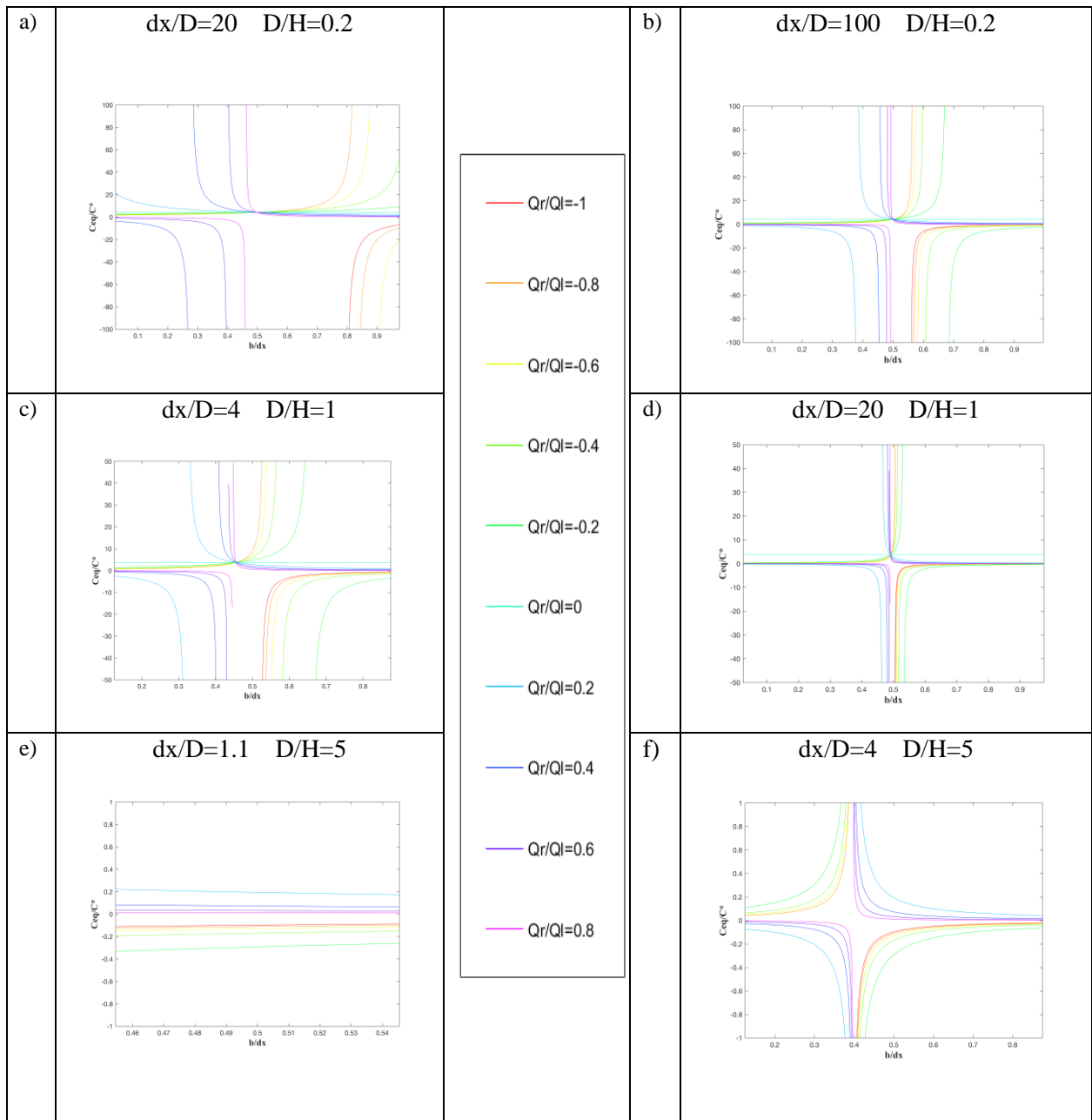


Figure 9. Effects of river position on equivalent parameter

4. Discussion and Recommendations

4.1. Effects of spatial discretisation on GW-SW exchange

Results of section 3.1 show that when surface water features, which are located in the centre of the cell, are of small river geometry, the effects of horizontal discretization are insignificant, i.e. errors are dominated by errors from neglecting the vertical flow. In such situations, one may consider refining the vertical discretization. Horizontal discretization was shown to have a considerable influence on errors compared to the error of vertical discretization, when the river is of greater width. In such situations, it is suggested that the modeller horizontally discretise the riverbed. The results showed that the errors are generally in greater values when the river and the underlying cell are of the same size, which might be due to inability of the numerical solution to capture the vertical flows occurring outside of the river cell.

Moreover, results of section 3.1 shows that refining the horizontal grid contribute to a more accurate exchange value; such that by refining the horizontal dimension of the streambed, the error values converge with a higher frequency and lower amplitude to a point that the errors from horizontal coarsening is insignificant. The results showed that even minor refinements of the riverbed can significantly reduce the error values.

Regarding the effect of river position, observations of section 3.2 show how different the errors can be depending on the position of the river in the cell, particularly when the discretization is large. Results also show that effects of river position are more influential for wider rivers. In instances where the river is close to borders of the river cell, errors of greater value are observed. These errors are probably due to the inability of the numerical solution to capture a majority of vertical flows. It is suggested that modellers avoid situations where river is very close to the cell border by considering it when choosing the grid size. Using an unstructured grid might also provide an additional flexibility.

The effects of river position can be significant when different version of a model are compared to each other. For instance, changing the horizontal resolution from 2km to 1km can significantly changes the spatial location of the river within a regional cell. The observed trends here may explain part of the grid resolution effects in the latest regional model of Adelaide Plains, South Australia (Bresciani et al 2015), in which some instances identified that fluxes fluctuate slightly when the model is being refined; however, those effects can also be the result of other parameters affected by grid resolution (e.g. imposed hydraulic heads in the RIV package), influence of which is not studied here and may be subject to future studies.

4.2. Suitability of the equivalent parameter approach

Results of section 3.3 and 3.4 show the variability of equivalent parameter in response to parameters such as river geometry, grid resolution, flow conditions and spatial position of the river within the cell. Anderson (2005) showed the variability of the equivalent parameter to flow conditions in the analytical context, but observations show different trends in the numerical setting. Dependence of the equivalent parameter on flow conditions, limit the prediction capability of the model only to the conditions for which it is calibrated. Spatial position of the river has not been studied before, but Figure 9 show that it has a strong influence on the equivalent conductance.

Furthermore, both Figure 8 and Figure 9 show that values of calibrated conductance become negative in some cases. Negative conductance values, however, are contradictory with the physical description of the riverbed conductance which is defined by positive parameters (Eq. 4). This discrepancy between the physical and calibrated conductance reflects the unsuitability of the approach for some river-aquifer arrangements. In previous studies, calibrated conductance was always reported to be in the range of positive values (Anderson, 2005, Rushton, 2007, Cousquer et al., 2017).

In practice, riverbed conductance is initially assigned by employing empirical values and achieved during the calibration process. When using a calibration software, modeller assigns lower and upper boundaries for riverbed conductance, and typically, one does not use negative values. Consequently, calibration process overlooks the scenarios in which calibrated conductance is calculated to be negative. If the modeller requires to use the clogging layer conceptualization, it is suggested that one extends the calibration boundaries to negative values. By doing such, occurrence of negative values may work as an indicator for situations where the clogging layer conceptualization is extremely unsuitable.

4.3. Limitations of the study

The conceptual model presented here, has been studied for a simplified case of a confined homogeneous aquifer being directly in contact with a river, in absence of any clogging layer, being modelled in 2-D cross-sectional extent. Therefore, the results are likely to vary in case of adoption of different initial assumptions.

4.4. Ways forward

The analytical solution provided by Morel-Seytoux et al. (2016) and the numerical approach of Cousquer et al. (2017) adopted the influence of a range of parameters, and in the future their method can be extended to include the effects of river position in the cell. Results of this study show that in cases of low drainage density, or lack of computational constraints, local grid refinement (Mehl and Hill, 2005) is likely to considerably increase the accuracy of the GW-SW problems. The two-parameter model of Anderson (2005) also shows promising results in neutralising the effects of flow conditions in the analytical context. However, their results need to be expanded and tested in the numerical context.

5. Conclusion

An exact analytical solution was used to investigate the errors originating from horizontal grid resolution in the current approach of modelling surface water features in groundwater flow models. Impact of the horizontal discretization was studied and showed that for narrow rivers error from horizontal discretization is negligible compared to the errors from vertical coarsening, while the opposite is true for the wide rivers. The influence of river position within the numerical model cell was studied and the results show that the location of the river can have a significant influence on the errors induced to the model, particularly if the river is closer to the borders of the cell.

The results show a strong dependence of the clogging layer conceptualization on several parameters, such as flow regimes, size of the grids, and spatial position of the river relative to the grid. Depending on the river and cell arrangements, the impacts of these parameters may introduce significant errors to the model. Due to complexity, the influences of these parameters are typically overlooked in practice and the exchange calculated through calibration. It is suggested that in the future the effects of these parameters are adopted to develop a more efficient conceptualization for calculating the GW-SW exchange. This study provides recommendations which may result in reduction of the identified errors.

References

- AESCHBACH-HERTIG, W. & GLEESON, T. 2012. Regional strategies for the accelerating global problem of groundwater depletion. *Nature Geoscience*, 5, 853-861.
- ANDERSON, E. I. 2005. Modeling groundwater-surface water interactions using the Dupuit approximation. *Advances in Water Resources*, 28, 315-327.
- ANDERSON, M. P., WOESSNER, W. W. & HUNT, R. J. 2015. Chapter 5 - Spatial Discretization and Parameter Assignment. *Applied Groundwater Modeling (Second Edition)*. San Diego: Academic Press.
- BARTHEL, R. & BANZHAF, S. 2016. Groundwater and Surface Water Interaction at the Regional-scale – A Review with Focus on Regional Integrated Models. *Water Resources Management*, 30, 1-32.
- BRUNKE, M. & GONSER, T. O. M. 1997. The ecological significance of exchange processes between rivers and groundwater. *Freshwater Biology*, 37, 1-33.
- BRUNNER, P., SIMMONS, C. T., COOK, P. G. & THERRIEN, R. 2010. Modeling surface water-groundwater interaction with MODFLOW: Some considerations. *Ground Water*, 48, 174-180.
- COUSQUER, Y., PRYET, A., FLIPO, N., DELBART, C. & DUPUY, A. 2017. Estimating River Conductance from Prior Information to Improve Surface-Subsurface Model Calibration. *Groundwater*, 55, 408-418.
- DE LANGE, W. J. 1999. A Cauchy boundary condition for the lumped interaction between an arbitrary number of surface waters and a regional aquifer. *Journal of Hydrology*, 226, 250-261.
- FENSKE, J. P., LEAKE, S. A. & PRUDIC, D. E. 1996. Documentation of a computer program (RES1) to simulate leakage from reservoirs using the modular finite-difference ground-water flow model (MODFLOW). *Open-File Report*. - ed.
- FLECKENSTEIN, J. H., KRAUSE, S., HANNAH, D. M. & BOANO, F. 2010. Groundwater-surface water interactions: New methods and models to improve understanding of processes and dynamics. *Advances in Water Resources*, 33, 1291-1295.
- GODERNIAUX, P., BROUYÈRE, S., FOWLER, H. J., BLENKINSOP, S., THERRIEN, R., ORBAN, P. & DASSARGUES, A. 2009. Large scale surface–subsurface hydrological model to assess climate change impacts on groundwater reserves. *Journal of Hydrology*, 373, 122-138.
- HAITJEMA, H. M. 1987. Comparing a three-dimensional and a Dupuit-Forchheimer solution for a circular recharge area in a confined aquifer. *Journal of Hydrology*, 91, 83-101.
- HARBAUGH, A. W. 2005. The US geological survey modular ground-water model - the ground-water flow process, US Geological Survey Techniques and Methods 6-A16.
- IRVINE, D. J., BRUNNER, P., FRANSSSEN, H.-J. H. & SIMMONS, C. T. 2012. Heterogeneous or homogeneous? Implications of simplifying heterogeneous streambeds in models of losing streams. *Journal of Hydrology*, 424–425, 16-23.
- KALBUS, E., REINSTORF, F. & SCHIRMER, M. 2006. Measuring methods for groundwater & surface water interactions: a review. *Hydrol. Earth Syst. Sci.*, 10, 873-887.
- LIGGETT, J. E., WERNER, A. D. & SIMMONS, C. T. 2012. Influence of the first-order exchange coefficient on simulation of coupled surface–subsurface flow. *Journal of Hydrology*, 414–415, 503-515.
- MEHL, S. & HILL, M. C. 2010. Grid-size dependence of Cauchy boundary conditions used to simulate stream-aquifer interactions. *Advances in Water Resources*, 33, 430-442.

- MEHL, S. W. & HILL, M. C. 2005. MODFLOW-2005, The US Geological Survey Modular Ground-Water Model - documentation of shared node local grid refinement and the boundary flow and head (BFH) package, US Geological Survey Techniques and Methods, 6-A12.
- MERRITT, M. L. & KONIKOW, L. F. 2000. Documentation of a computer program to simulate lake-aquifer interaction using the MODFLOW ground water flow model and the MOC3D solute-transport model. *Water-Resources Investigations Report*. - ed.
- MIRACAPILLO, C. & MOREL-SEYTOUX, H. J. 2014. Analytical solutions for stream-aquifer flow exchange under varying head asymmetry and river penetration: Comparison to numerical solutions and use in regional groundwater models. *Water Resources Research*, 50, 7430-7444.
- MOREL-SEYTOUX, H. J. 2009. The turning factor in the estimation of stream-aquifer seepage. *Ground Water*, 47, 205-212.
- MOREL-SEYTOUX, H. J., MEHL, S. & MORGADO, K. 2014. Factors influencing the stream-aquifer flow exchange coefficient. *Groundwater*, 52, 775-781.
- MOREL-SEYTOUX, H. J., MILLER, C. D., MIRACAPILLO, C. & MEHL, S. 2016. River Seepage Conductance in Large-Scale Regional Studies. *Groundwater*.
- OLSTHOORN, T. N. 2013. User guide for mflab. *Delft University of Technology, Waternet*.
- PAUW, P. S., VAN DER ZEE, S. E. A. T. M., LEIJNSE, A., DELSMAN, J. R., DE LOUW, P. G. B., DE LANGE, W. J. & OUDE ESSINK, G. H. P. 2015. Low-Resolution Modeling of Dense Drainage Networks in Confining Layers. *Groundwater*, 53, 771-781.
- PRUDIC, D. E. 1989. Documentation of a computer program to simulate stream-aquifer relations using a modular, finite-difference, ground-water flow model. *Open-File Report*. - ed.
- PRUDIC, D. E., KONIKOW, L. F. & BANTA, E. R. 2004. A New Streamflow-Routing (SFR1) Package to Simulate Stream-Aquifer Interaction with MODFLOW-2000. *Open-File Report*. - ed.
- RASSAM, D. & WERNER, A. 2008. Review of groundwater-surface water interaction modelling approaches and their suitability for Australian conditions. *eWater Cooperative Research Centre, Canberra*.
- RUSHTON, K. 2007. Representation in regional models of saturated river-aquifer interaction for gaining/losing rivers. *Journal of Hydrology*, 334, 262-281.
- SNOWDON, A. P. & CRAIG, J. R. 2016. Effective groundwater-surface water exchange at watershed scales. *Hydrological Processes*, 30, 1849-1861.
- SOPHOCLEOUS, M. 2002. Interactions between groundwater and surface water: The state of the science. *Hydrogeology Journal*, 10, 52-67.
- VERMEULEN, P. T. M., TE STROET, C. B. M. & HEEMINK, A. W. 2006. Limitations to upscaling of groundwater flow models dominated by surface water interaction. *Water Resources Research*, 42.
- VILHELMSSEN, T. N., CHRISTENSEN, S. & MEHL, S. W. 2012. Evaluation of MODFLOW-LGR in connection with a synthetic regional-scale model. *Ground Water*, 50, 118-132.
- WINTER, T. C. 1999. Relation of streams, lakes, and wetlands to groundwater flow systems. *Hydrogeology Journal*, 7, 28-45.
- WINTER, T. C., HARVEY, J. W., FRANKE, O. L. & ALLEY, W. M. 1998. Ground water and surface water; a single resource. *Circular*. - ed.
- ZHOU, Y. & LI, W. 2011. A review of regional groundwater flow modeling. *Geoscience Frontiers*, 2, 205-214.

Appendix

Mflab Script

```
clearvars

H = 1;
K=1e-4;
hriver=1.1;
hl_exact=1.3;
D = (1*H);
gamma=exp(-pi*(D/H));
r= [1 0 -1];
dx_values= [0.001:0.001:0.002] *D;
min_L_physical=2*H;
min_L=2*H;

for ir= 1: length(r)

    Ql=(hl_exact-hriver)./(min_L_physical/(K*H)+r(ir)/(K*pi))*log((1-
gamma.^0.5)./(1+gamma.^0.5))-1/(K*pi)*log(0.25*(1-gamma)));
    Qr= r(ir)*Ql;
    for idxx=1: length(dx_values)
        dx=dx_values(idxx);

        % Location of the river within the cell
        b=0.5*dx;

        % Number of river cells on the left of centre cell
        Nriv_left = ceil((0.5*D-b)/dx);

        % Number of river cells on the right of centre cell
        Nriv_right = ceil((0.5*D-dx+b)/dx);

        % Total of river cells (1 is for the centre cell)
        Nriv = Nriv_left + 1 + Nriv_right;

        % Distance from right river edge to cell border (lr)
        lr = (Nriv_right+1) *dx-b-0.5*D;

        % Number of cells to add on the right to satisfy min_L (Nr)
        % This means lr+(Nr-0.5) *dx >= min_L
        % This means Nr >= (min_L-lr)/dx+0.5
        Nrc = ceil((min_L-lr)/dx+0.5);
        Nr=max(Nrc,1);

        % Distance from left river edge to cell border (ll)
        ll = (Nriv_left) *dx+b-0.5*D;
```

```

% Number of cells to add on the left to satisfy min_L (Nl)
% This means  $l_1+(Nl-0.5) *dx \geq min\_L$ 
% This means  $Nl \geq (min\_L-l_1)/dx+0.5$ 
Nlc = ceil((min_L-l1)/dx+0.5);
Nl= max(Nlc,1);

% Length at which heads are calculated
Lexact=lr+(Nr-0.5) *dx;

mf_setup; % mf_setup is defined in a separate mfile
load('First.mat')
load('First')

head = readDat(['First','','. hds']);
hl_numerical(idxx, ir) = head.values(1);
hr_numerical(idxx, ir) = head.values(end);

hr_exact(idxx, ir)=(-Qr*Lexact/(K*H))+Qr/(K*pi).*log(0.25*(1-gamma))-
Ql/(K*pi).*log((1-gamma.^0.5)./(1+gamma.^0.5))+hriver;

end
end

```

```

err=(hr_numerical- hr_exact)./(hl_exact-hriver)*100;

plot(dx_values,err);

```

mf_setup:

```

% Calling for packages and solvers

basename = 'First';

% building the model resolution

xGr= -dx*Nl: dx:1.0000001*dx*(Nriv+Nr);
yGr= [0 1];
zGr= [H 0];

[xGr, yGr, zGr, xm, ym, zm, Dx, Dy, Dz, Nx, Ny, Nz]=modelsize3(xGr, yGr, zGr);
gr = gridObj(xGr, yGr, zGr);

% assigning the initial conditions
HK = gr.const(K);
VK = K;

IBOUND = gr.const(1);

```

```

STRTHD = gr.const(H);

% Defining the river cells and their parameters

sp_number = ones(Nriv,1);
layer_number = ones(Nriv,1);
row_number = ones(Nriv,1);
column_number = [Nl+1:1: Nl+Nriv]';
HRIV = hriver*ones(Nriv,1);

CRIV = nan(Nriv,1);
if Nriv==1
    CRIV (1,1) = 2*K*D/H;
else
    CRIV (1,1) = 2*K*(dx-ll)/H;
    CRIV(Nriv,1) = 2*K*(dx-lr)/H;
    if Nriv>2
        CRIV (2: Nriv-1,1) = 2*K*dx/H;
    end
end

RBOT = 0.001*ones(Nriv,1);
RIV = [sp_number, layer_number, row_number, column_number, HRIV, CRIV, RBOT];

% Defining the wells and their parameters

well (1) = wellObj(1, -dx*Nl+dx/2,0.5,0,1,.15);
well (1). Q = Ql;

well (2) = wellObj(2, (Nr+Nriv)*dx-dx/2,0.5,0,1,.15);
well (2). Q = -Qr;

well = well.toGrid(gr,HK);

```